Decoherence and dephasing in strongly driven colliding Bose-Einstein condensates

N. Katz, R. Ozeri, E. Rowen, E. Gershnabel, and N. Davidson
Department of Physics of Complex Systems, Weizmann Institute of Science, Rehovot 76100, Israel
(Received 7 May 2004; revised manuscript received 24 June 2004; published 30 September 2004)

We report on a series of measurements of decoherence and wave-packet dephasing between two colliding, strongly coupled, identical Bose-Einstein condensates. We measure, in the strong-excitation regime, a suppression of the mean-field shift, compared to the shift which is observed for a weak excitation. This suppression is explained by applying the Gross-Pitaevskii energy functional. By selectively counting only the nondecohered fraction in a time-of-flight image we observe oscillations for which both inhomogeneous and Doppler broadening are strongly suppressed. If no post-selection is used, the decoherence rate due to collisions can be extracted and is in agreement with the local density average calculated rate.

DOI: 10.1103/PhysRevA.70.033615 PACS number(s): 03.75.Kk, 03.75.Lm, 32.80.−t

I. INTRODUCTION

Decoherence of a quantum system typically involves the coupling of an excitation to a continuum of fluctuating modes. The random initial phases of these modes lead to an effective irreversibility on time scales larger than the so-called "memory time" of the system [1]. The coherent part of the system's evolution, although possibly nonlinear, is inherently reversible and therefore any observed decay due to this evolution is typically termed as dephasing. The ability to distinguish between these two decay mechanisms and to limit their effects is of great importance to quantum control and manipulation.

The dephasing of a momentum excitation in a nonuniform Bose-Einstein condensate (BEC) is governed by several factors [2,3], notably, the inhomogeneous broadening of the Bogoliubov energy spectrum and the Doppler broadening. We denote these processes as dephasing since they involve a reversible, although nonlinear, evolution of a macroscopic condensate wave function. In contrast, the decoherence of such an excitation due to collisions with the BEC involves coupling to a quasicontinuum of initially unoccupied momentum states [4].

In previous works the inhomogeneous line shape was seen to agree, for short Bragg coupling times, with both the experimental data [5,6] and with simulations of the Gross-Pitaevskii equation (GPE) [7]. At longer time scales the inhomogeneous line shape is resolved into radial modes [6]. Weak-probe Bragg spectroscopy and interferometry were also used to characterize the coherence and spatial correlation function of condensates [8] and quasicondensates [9]. These works found that the spatial coherence of three-dimensional condensates is Heisenberg limited, while the coherence of one-dimensional condensates is significantly degraded by the stronger effective interaction.

In this paper we measure the dephasing and decoherence of strongly driven oscillations between two identical colliding BEC's. By post-selecting the nondecohered fraction we observe a strong suppression of both inhomogeneous and Doppler broadening mechanisms, resulting in a corresponding order of magnitude increase in the dephasing time. This long dephasing time is found to be in surprising quantitative agreement with the results of a GPE simulation, even for rather small (<0.25) nondecohered fraction. We surmise that the decohered excitations exert a mean field that does not alter the coherent evolution significantly during the time scale of our experiment. Thus we find that the effects of dephasing can be distinguished from those of decoherence via post-selection. Using the calculated and measured dephasing rate we can also determine the observed collisional decoherence rate and it is seen to agree with the local density approximation (LDA) average of the free particle collision rate.

II. MODEL FOR STRONG EXCITATIONS

For comparison with the results for strong excitations, we first briefly review the main broadening mechanisms for perturbative Bragg excitations. The rms width of the LDA inhomogeneous line shape for weak high-momentum excitations is given by $\sqrt{8/147}\,\mu$, where μ is the chemical potential of the BEC [2]. The rms Doppler broadening is given by $\sqrt{8/3}\hbar k/mR_z$ [2], where k is the wave number of the excitation, m is the mass of the BEC atom, and R_z is the Thomas-Fermi radius of the condensate. For our experimental parameters the Doppler dephasing rate is predicted to be 0.6 kHz and is clearly dominated by the expected 3.0 kHz inhomogeneous dephasing rate [11].

In the case of a strong excitation the population of the zero-momentum condensate is significantly depleted and transferred coherently to a traveling condensate in a Rabi-like oscillation. In order to clarify the physics behind such strong excitations in BEC, we introduce an effective two-level system between the zero momentum state and the excitation state. For large k we approximate such strongly excited mixed states by $\psi(r,z)=a\phi_0(r,z)+be^{ikz}\phi_0(r,z)$ [12], where a and b are the amplitudes of the effective two-level system. The total number of atoms, N, is constant and equal to $|a|^2+|b|^2$. Here $\phi_0(r,z)$ is the ground-state wave function of the system with no excitations.

The energy of such a state ψ can be evaluated by the Gross-Pitaevskii energy functional [13] $E=\int dV\{(\hbar^2/2m)|\nabla\psi(r,z)|^2+V_0(r,z)|\psi(r,z)|^2+(g/2)|\psi(r,z)|^4\}$, where V_0 is the external potential and g is the mean-field coupling constant. By differentiating the energy by the ex-

cited state population $N_k=|b|^2$, and considering the result as a function of N_k, we find a population-dependent excitation energy

$$\epsilon_k(N_k)=\frac{\hbar^2k^2}{2m}+\left(1-\frac{2N_k}{N}\right)\mu, \tag{1}$$

where $\mu=gn$, with n the density of the condensate. At low N_k our model recovers the perturbative excitation Bogoliubov energy for high-k excitations. When N_k approaches N the mean-field shift is negative, since the mean-field interference between the zero-momentum state and the k state is being removed. The intuitive picture is that the energy per particle required to transfer the condensate from $N_k=0$ to $N_k=N$ is simply the free particle energy, since the internal interaction energy is not changed by such a transformation. At sufficiently large Rabi frequencies that achieve complete population inversion, the temporary mean-field detuning averages in time to zero due to the symmetry around the $N/2$ point. Thus the resonance for such strong excitations is expected to shift to the free particle value.

Since the excitation energy is population dependent, an initially on-resonance weak Bragg coupling will be shifted out of resonance as population is accumulated in the excitation. Consequently, the system will not achieve population inversion. Such an effect is generally referred to as population trapping [7,10].

At the intermediate regime, where the strength of Rabi driving potential is equal to one-half of the Bogoliubov shift, quantum backreaction effects, beyond the mean field, are expected for a simple two-mode many-body system [10]. Indeed, our GPE simulations [14], with parameters as in the experiment described below, indicate a strong inherent instability at this Rabi frequency ($\sim$0.7 kHz). The instability manifests as a rapid dispersion of the excitations out of the two coupled momentum modes, which is not possible in the closed two modes of [10]. Thus the GPE simulation indicates its own loss of validity at this point [15]. Further studies of this system using more advanced techniques, such as the stochastic GPE method [16], are necessary in order to better explain this nontrivial system.

III. EXPERIMENT

Our experimental apparatus is described in [17]. Briefly, a nearly pure (>90%) BEC of $1.6(\pm0.5)\times10^5$ ^{87}Rb atoms in the $|F,m_f\rangle=|2,2\rangle$ ground state is formed in a cylindrically symmetric magnetic trap, with radial ($\hat{r}$) and axial ($\hat{z}$) trapping frequencies of $2\pi\times226$ Hz and $2\pi\times26.5$ Hz, respectively. This corresponds to $\mu/h=2.48$ kHz. We excite the condensate at a well-defined wave number using two-photon Bragg transitions [18]. The two Bragg counterpropagating (along $\hat{z}$) beams are locked to a Fabry-Perot cavity line, detuned 44 GHz below the $5S_{1/2},F=2\rightarrow5P_{3/2},F'=3$ transition. At this detuning and at the intensities used here, there are no discernable losses from the condensate due to spontaneous emission. Bragg pulses of variable duration and intensity are applied to the condensate, controlling the excitation process.

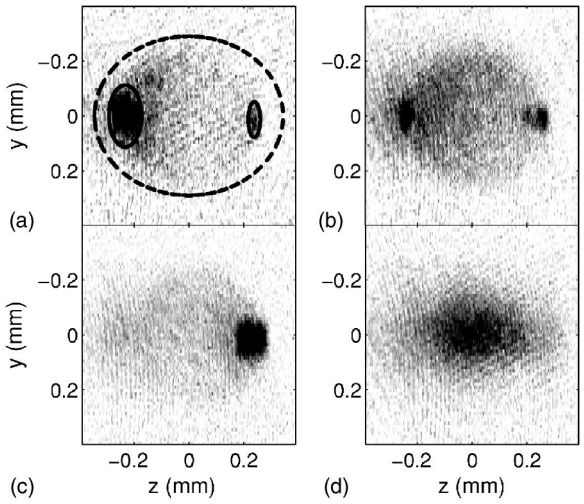

FIG. 1. Time of flight images of oscillating and colliding BEC's. (a) A weak perturbation of the BEC (left, in solid line ellipse) to the excited population (right, in solid line ellipse). The dashed line marks the region of interest for measuring the average momentum P_{tot}. (b) A $\pi/2$ pulse. Note the strong collisional sphere. (c) Almost a π pulse. Note the weak collisional sphere, indicating collisions between the excitation and the zero-momentum BEC. (d) After further oscillation ($>10\pi$ at 8.6 kHz), the BEC's are completely decohered, and the Bragg coupling no longer effects the system.

Immediately after the Bragg pulse, the magnetic trap is rapidly turned off, and after a 38 msec of time-of-flight expansion the atomic cloud is imaged by an on-resonance absorption beam, perpendicular to the $\hat{z}$ axis. Figure 1 shows the resulting absorption images, for different excitation strengths and duration. Figure 1(a) shows a perturbative excitation with the large cloud at the left corresponding to the BEC. A halo of scattered atoms is visible between the BEC and the cloud of unscattered outcoupled excitations to the right. In Fig. 1(b) we show a $\pi/2$ pulse which generates a nearly symmetric excitation in momentum space. The two condensates collide producing a strong collisional sphere. In Fig. 1(c) we show a nearly complete π pulse. We note the weak thermal cloud surrounding the origin, which is largely unaffected by the Bragg pulse. When we increase the duration time of Rabi oscillations [Fig. 1(d)], the effective two-level system is eventually depleted by collisions.

Following [19], we measure the response of our system by integrating over the elliptical areas shown in Fig. 1(a). The solid lines are Gaussian fit areas to the unscattered atoms. The dashed line contains the entire region of interest, including the collisional products. We define the number of atoms observed in the excited region enclosed in the ellipse to the right as N_k and those corresponding to the initial BEC to the left as N_0. Here P_{tot} is the total momentum in units of the momentum of a single excitation along $\hat{z}$ measured inside the dashed ellipse and normalized by the overall number of observed atoms.

The suppression of the mean-field shift in strongly excited condensates is shown in the spectrum of Fig. 2(b), where the resonance is clearly (14.9 ± 0.2 kHz from a Gaussian fit) in agreement with the free particle value of 15.08 kHz, indicated by the dotted line. This should be compared to the

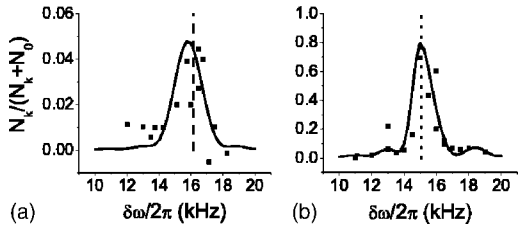

FIG. 2. Measured Bragg response (solid boxes) spectroscopy ($N=0.9\times10^5$ and pulse duration of 0.5 msec for these measurements). Solid lines are GPE simulations. (a) Weak-excitation spectrum exhibiting the usual mean-field shifted Bogoliubov excitation resonance. The dashed line is at the theoretical LDA excitation energy (16.15 kHz). (b) Strong-excitation spectrum, in which a clear suppression of the mean-field shift is observed. The dotted line is at the free particle excitation energy (15.08 kHz).

resonance (16.05 ± 0.2 kHz from a Gaussian fit) observed in Fig. 2(a) for a weak excitation in agreement with the expected LDA Bogoliubov value of 16.15 kHz indicated by the dashed line. The solid lines are GPE simulations of the system, which also confirm the suppression of the mean-field shift.

This suppression of the mean-field shift should cause a similar decrease in the inhomogeneous broadening, leading to longer coherence times for strongly driven condensates. We explore this at various driving Rabi frequencies while holding $\delta\omega=2\pi\times15$ kHz constant at the free particle excitation energy. Figures 3(a) and 3(b) show $P_{tot}(t)$ at the driving frequencies of 1.2 kHz and 8.6 kHz, respectively. Figures 3(c) and 3(d) show $N_k/(N_0+N_k)(t)$, for the same driving frequencies.

The dashed lines in Figs. 3(a) and 3(b) are exponentially decaying oscillations, fitted to the experimental points. Here the decay is mainly due to collisions between the two condensates. The solid lines in Figs. 3(c) and 3(d) are GPE simulations with no fit parameters. We observe the remarkable result that by studying the dynamics of $N_k/(N_0+N_k)(t)$ we recover the GPE dephasing behavior, despite the fact that the GPE does not include collisions between excitations and considers only the evolution of the macroscopic wave function. We surmise that the decohered excitations continue to exert a mean field that does not significantly degrade the continued coherent evolution of the nondecohered fraction. At high momentum, the mean field felt by the coherent fraction depends mainly on the density distribution of the system, which evolves on a time scale longer than the experiment. This is reminiscent of internal state excitation dephasing and decoherence studied by rf spectroscopy [20].

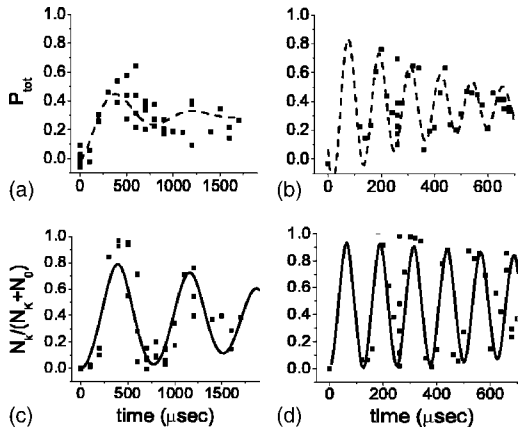

FIG. 3. Experimental oscillations between two coupled BEC's (solid boxes). Average momentum P_{tot} at 1.2 (a) and 8.6 (b) kHz oscillations. The oscillations are damped due to collisions. The dashed lines in (a) and (b) are exponentially decaying oscillation fits to the points. Post-selection of the uncollided fraction $N_k/(N_0+N_k)$ for the 1.2 (c) and 8.6 (d) kHz oscillations. The solid lines in (c) and (d) are GPE simulations with no fitting parameters.

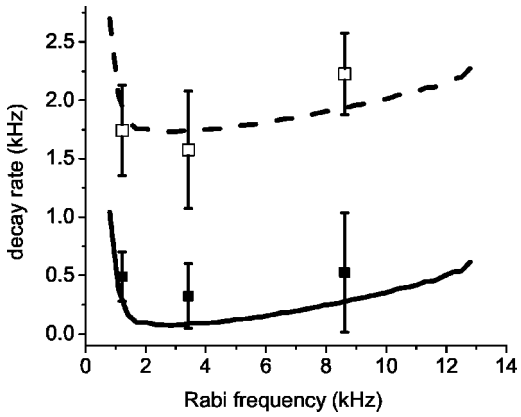

FIG. 4. Measured decay rates as a function of oscillation frequency. The solid boxes are the exponential fit decay rates of the oscillations in the post-selected $N_k/(N_0+N_k)$. The solid line is the rate of decay fitted to the results of GPE simulations. The open boxes are the fitted decay rates of average momentum P_{tot}. The dashed line is the sum of the expected LDA collision rate (1.66 kHz) with the decay rates from GPE simulations (solid line).

The results are summarized in Fig. 4. Here the solid boxes show the measured dephasing decay rate of $N_k/(N_0+N_k)(t)$. An additional experimental point is measured at the Rabi driving frequency of 3.4 kHz. The solid line represents the theoretical dephasing rate obtained by numerically solving the GPE and then fitting the time evolution to an oscillating exponential decay.

The open boxes are the fitted decay rate of the oscillations in $P_{tot}(t)$. The dashed line is the result of the theoretical sum of the GPE dephasing rate calculated above (solid line), plus the free particle LDA collision rate (1.66 kHz) [21], with no fitting parameters.

There are several points of interest in this figure. First, we note that the prediction of our simple model—i.e., suppression of dephasing—is again confirmed both in simulation and in experiment. The simulation indicates, at the Rabi driving frequency of ~3 kHz, a 30-fold increase in the expected dephasing time relative to that of a perturbative excitation [2]. A GPE simulation, with our experimental parameters, of a weak-excitation Ramsey experiment confirms the rapid dephasing of perturbative excitations and agrees with the simplified expressions of [2].

Experimentally, at the ~3 kHz driving Rabi frequency, the observed decay rates of P_{tot} and $N_k/(N_0+N_k)$ are 2 and 10 times smaller, respectively, than the calculated inhomoge-

neous dephasing rate. At this point the decay rate of $N_k/(N_0+N_k)$ (0.3 kHz) lies almost 9σ from the perturbative excitation decay rate (3.1 kHz).

At lower driving frequencies, we observe that the GPE simulation predicts a sharp increase in decay rate for lower driving frequencies. In the terms of our two-mode model, this represents a population trapping [7] of nonlinear Rabi oscillations that is not suppressed for these low driving frequencies. At the limit of perturbative excitations, the simplified calculated dephasing rates of [2] are again recovered.

Second, the GPE simulation dephasing rate ($\sim$0.1 kHz) near 3 kHz driving frequency is significantly slower than the Doppler dephasing rate (0.6 kHz). The experimental points agree with this trend. This suppression can be understood by considering the system in the frame of reference of the traveling light potential [22]. In this reference frame the condensate is on the edge of the Brillouin zone and is repeatedly reflected by the potential. Due to the strong lattice potential, there is a broad region in momentum space for which the group velocity is zero. The Doppler broadening is proportional to the energy uncertainty of the condensate due to its momentum spread and is calculated using the excitation spectrum. In a strong optical lattice the momentum spread no longer corresponds to an energy spread since the group velocity is zero. Consequently the Doppler broadening is also suppressed and in the time domain the two wave packets do not separate.

For driving Rabi frequencies much larger than 3 kHz our GPE simulations predict a monotonic increase of the decay rate of the system. The reason for this increase of the decay rate simulation appears to result from the excitation of other momentum modes along with residual wave-packet spreading in momentum space.

Finally, we find that by subtracting the measured decay rate of $N_k/(N_0+N_k)(t)$ from that of $P_{tot}(t)$ we can isolate and estimate the decay due to collisions. We thus measure the collisional cross section to be $7.1(\pm 1.8)\times 10^{-16}$ m^2 in agreement with the known [21] value of 8.37×10^{-16} m^2 [23].

IV. CONCLUSION

In conclusion, we measure a suppression of the mean-field shift for a strong excitation of the BEC. We also observe an order of magnitude suppression of the inhomogeneous broadening and Doppler broadening mechanisms between strongly driven colliding Bose-Einstein condensates as compared to weakly excited condensates. This suppression leads to a corresponding order-of-magnitude increase in the coherence time of the system. Furthermore, we measure a collisional decoherence rate in agreement with that expected from previous measurements.

As a result of the strong coherent oscillations in the time domain, we expect a splitting both in a Bragg probe spectrum and in the collisional products analogous to the Mollow splitting [24]. In the future we also hope to measure a shift in the energy of the excitations due to off-resonance Bragg pulses, in analogy with the ac Stark shift. This shift may even modify the decoherence rate by shifting the resonance energy sufficiently to influence the interaction with the finite width collisional quasicontinuum [25]. In addition, we also hope to observe further nontrivial decoherence mechanisms [10] as indicated by numerical GPE instability at specific driving frequencies.

ACKNOWLEDGMENTS

This work was supported in part by the Israel Ministry of Science, the Israel Science Foundation, and the Minerva Foundation.

[1] C. Cohen-Tannoudji, J. Dupont-Roc, and G. Grynberg, *Atom-Photon Interactions* (Wiley, New York, 1992).

[2] F. Zambelli, L. Pitaevskii, D. M. Stamper-Kurn, and S. Stringari, Phys. Rev. A **61**, 063608 (2000).

[3] J. Stenger, S. Inouye, A. P. Chikkatur, D. M. Stamper-Kurn, D. E. Pritchard, and W. Ketterle, Phys. Rev. Lett. **82**, 4569 (1999).

[4] N. Katz, J. Steinhauer, R. Ozeri, and N. Davidson, Phys. Rev. Lett. **89**, 220401 (2002).

[5] D. M. Stamper-Kurn, A. P. Chikkatur, A. Gorlitz, S. Inouye, S. Gupta, D. E. Pritchard, and W. Ketterle, Phys. Rev. Lett. **83**, 2876 (1999).

[6] J. Steinhauer, N. Katz, R. Ozeri, N. Davidson, C. Tozzo, and F. Dalfovo, Phys. Rev. Lett. **90**, 060404 (2003).

[7] A. Brunello, F. Dalfovo, L. Pitaevskii, S. Stringari, and F. Zambelli, Phys. Rev. A **64**, 063614 (2001).

[8] E. W. Hagley, L. Deng, M. Kozuma, M. Trippenbach, Y. B. Band, M. Edwards, M. Doery, P. S. Julienne, K. Helmerson, S. L. Rolston, and W. D. Phillips, Phys. Rev. Lett. **83**, 3112 (1999); M. Trippenbach, Y. B. Band, M. Edwards, M. Doery, P. S. Julienne, E. W. Hagley, L. Deng, M. Kozuma, K. Helmerson, S. L. Rolston, and W. D. Phillips, J. Phys. B **33**, 47 (2000).

[9] S. Richard, F. Gerbier, J. H. Thywissen, M. Hugbart, P. Bouyer, and A. Aspect, Phys. Rev. Lett. **91**, 010405 (2003); D. Hellweg, L. Cacciapuoti, M. Kottke, T. Schulte, K. Sengstock, W. Ertmer, and J. J. Arlt, *ibid.* **91**, 010406 (2003).

[10] A. Vardi and J. R. Anglin, Phys. Rev. Lett. **86**, 568 (2001).

[11] For concreteness we denote the dephasing time by the $1/e$ decay time of the cosine transform of the line shape. The dephasing rate is the inverse of the dephasing time. This corresponds to an analytical estimate of the decay rate of the Ramsey fringes and is confirmed numerically by simulating the dephasing of a Ramsey-type experiment using cylindrically symmetric GPE [14].

[12] M. G. Moore and P. Meystre, Phys. Rev. Lett. **83**, 5202 (1999).

[13] C. Cohen-Tannoudji and C. Robilliard, C. R. Acad. Sci., Ser IV: Phys., Astrophys. **2**, 445 (2001).

[14] We numerically solve the GPE for the order parameter of the

condensate $i\hbar\partial_t\psi=\{-\hbar^2\nabla^2/2m+V+g|\psi|^2\}\psi$, with the time-dependent external potential typically of the form $V(\mathbf{r},t)=m/2(\omega_r^2r^2+\omega_z^2z^2)+\Omega(t)V_B\cos(kz-\delta\omega t)$. V_B is the two-photon Rabi Bragg frequency, and $\Omega(t)$ is a general envelope function. All other parameters for the simulation are as in the experimental system, described above. The ground state is found for $t<0$ by imaginary time evolution. We exploit the cylindrical symmetry to evolve the wave function on a two-dimensional grid $N_z\times N_r(4096\times 32)$, using the Crank-Nicholson differencing method along with the alternating direction implicit algorithm.

[15] S. Burger, F. S. Cataliotti, C. Fort, F. Minardi, M. Inguscio, M. L. Chiofalo, and M. P. Tosi, Phys. Rev. Lett. **86**, 4447 (2001).

[16] A. A. Norrie, R. J. Ballagh, and C. W. Gardiner, e-print cond-mat/0403378.

[17] J. Steinhauer, R. Ozeri, N. Katz, and N. Davidson, Phys. Rev. Lett. **88**, 120407 (2002).

[18] M. Kozuma, L. Deng, E. W. Hagley, J. Wen, R. Lutwak, K. Helmerson, S. L. Rolston, and W. D. Phillips, Phys. Rev. Lett. **82**, 871 (1999).

[19] A. P. Chikkatur, A. Gorlitz, D. M. Stamper-Kurn, S. Inouye, S. Gupta, and W. Ketterle, Phys. Rev. Lett. **85**, 483 (2000).

[20] D. M. Harber, H. J. Lewandowski, J. M. McGuirk, and E. A. Cornell, Phys. Rev. A **66**, 053616 (2002).

[21] H. M. J. M. Boesten, C. C. Tsai, J. R. Gardner, D. J. Heinzen, and B. J. Verhaar, Phys. Rev. A **55**, 636 (1997).

[22] M. Krämer, C. Menotti, L. Pitaevskii, and S. Stringari, e-print cond-mat/0305300.

[23] For weak excitations, at our experimental parameters, we expect a significant suppression of the collisional cross section as compared to the free particle value [4] ($\sim$351). However, for strong excitations we do not expect such a large suppression, since the perturbative assumptions do not apply.

[24] E. Rowen, N. Katz, R. Ozeri, E. Gershnabel, and N. Davidson, e-print cond-mat/0402225.

[25] A. G. Kofman and G. Kurizki, Phys. Rev. Lett. **87**, 270405 (2001).